Analysis of the trajectory of insulating particles in a free fall electrostatic separator with four vertical cylindrical electrodes

S. Touhami[1], W. Aksa[1], M. Maamar[1], T. Zeghloul[2], K. Medles[2], L. Dascalescu[2]

[1] Electrostatics and High Voltage Research Unit IRECOM,
University Djillali Liabes Sidi Bel Abbès 22000, Algeria

[2] Electrostatics of Dispersed Media Research Unit, Institut P', UPR 3346 CNRS-
University of Poitiers-ENSMA, Angoulême 16021, France

phone: (213) 555-115-045
e-mail: seddik.touhami@gmail.com

Abstract—**This paper presents an analysis of the trajectory of ABS and PVC particles in a free fall electrostatic separator. The installation that is the subject of this study is equipped with four vertical cylindrical electrodes. The behavior of the particles in this installation is compared with the behavior of the particles in a conventional configuration represented by two flat electrodes. The trajectory of the particles in both configurations is obtained by the numerical resolution of the Newton equation. The motion equation used in this study takes into account the intensity and direction of the electrostatic, gravitational and aerodynamic forces applied to the particles in the electrostatic separation zone. The calculation of the electrostatic force applied to the particles in this zone is performed using a numerical model of the electrostatic field obtained by finite element method implemented in the PDE-tool library of the MATLAB software. The results of this study show that the use of a four-electrode configuration reduces the quality deterioration of recovered products caused by the appearance of impacts between particles and electrodes observed in a conventional installation. But, the use of the new configuration requires the development of a collector the shape of which is adapted to the spatial distribution of the particles recovered at the outlet of the installation.**

Key words — **Simulation, Electrostatic Separator, Particle Trajectory.**

I. INTRODUCTION

In a free fall electrostatic separator [1-4], the sorting of granular mixtures recovered from a waste of electrical and electronic equipment is carried out by the action of the electrostatic forces applied to the particles of the mixture initially charged by triboelectric effect [5-9]. In a conventional installation (Figure.1.a), the particles of the granular mixture recovered at the outlet of a triboelectric device are introduced continuously into the space delimited by two flat electrodes parallel to a vertical plane. In this zone the charged particles are attracted to the electrodes of opposite polarities.

The theoretical study of the trajectory of particles in this configuration [10-14] shows that when applying an intense electrostatic field impacts may occur between the highly charged particles and the electrodes of the separator. In most cases, the impact of a particle with the electrode is followed by a projection of the particle into .
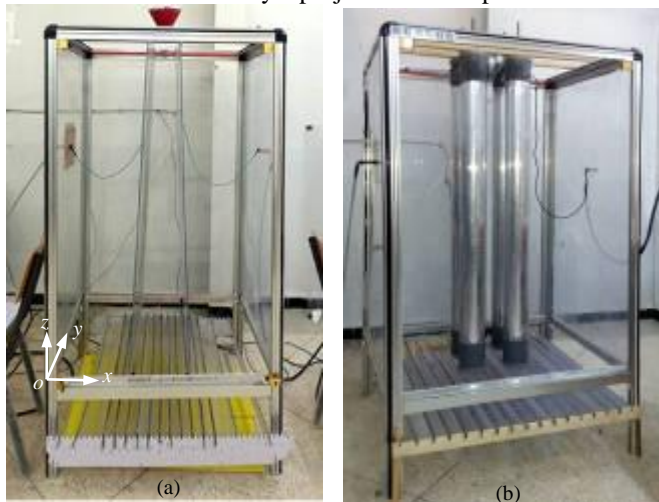

Fig. 1. Free-fall separator equipped with: (a) flat electrodes; (b) cylindrical electrodes.

The occurrence of this type of undesirable behavior during the separation reduces considerably the purity of the products recovered at the collector of the installation. To reduce the number of impacts, two solutions have been proposed.

The first solution is represented by the use of a configuration of inclined flat electrodes. This solution has been the subject of several theoretical and experimental studies which confirm the interest of the inclination of the electrodes in controlling the trajectory of the particles in the electrostatic separation zone [12].

The second solution is represented by the use of four cylindrical electrodes [13]. In this paper, a numerical model of the particle trajectory implemented under MATLAB is used in the analysis of the dynamic behavior of particles in this configuration. This model takes into account the stochastic nature of particle size, mass and charge as well as other parameters related to particle kinematics at the inlet of the separator. Validation of the simulation results is carried out performing an electrostatic separation experiment and measuring the position of the particles in the collector as a function of their charges and their masses.

II. Numerical Model

A. Electrostatic field model

The development of a particle trajectory simulation model in an electrostatic separation process requires information on the intensity and direction of the electrostatic field in the separation zone. In this paper, the model of the electrostatic field in both configurations is obtained by solving the Laplace equation (1) using the finite element method.

$$\frac{\partial^2 U}{\partial x^2} + \frac{\partial^2 U}{\partial y^2} + \frac{\partial^2 U}{\partial z^2} = 0 \tag{1}$$

A particular solution of the problem (1) is shown in figure 2. The solution obtained satisfies the Dirichlet boundary conditions imposed on the surface of the electrodes ($U = \pm 15$ kV) and the walls of the separation chamber ($U = 0$ kV). The same figure represents the electric potential in a plane $z = -L/2$ [m] where L [m] is the length of the electrodes of the installation. The black curves superposed on the potential distribution represent the electrostatic field lines calculated from the electrical potential by a numerical resolution of the equation:
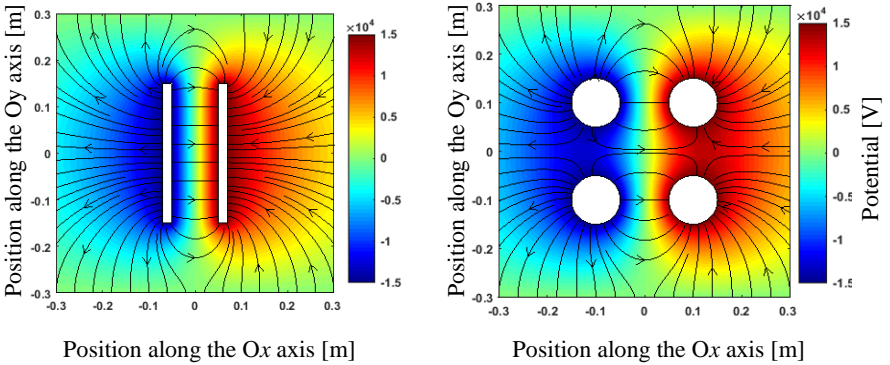
$$\vec{E} = -\vec{\nabla}U \tag{2}$$

Fig. 2. Potential and electrostatic field lines in: (a) a flat electrode separator and (b) a cylindrical electrode separator
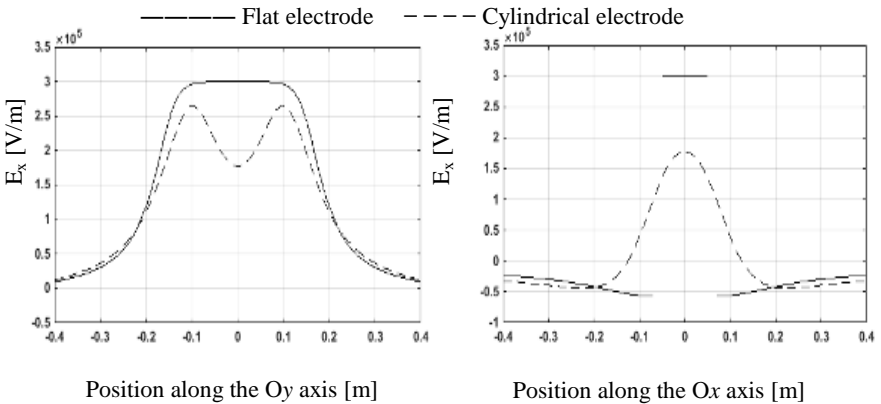

Fig. 3. Variation of the *Ex* component of the following electrostatic field: (a) O*y* axis and (b): O*x* axis

The analysis of the results shows that the value of the potential as well as the intensity and the direction of the electrostatic field in the set of planes $z = 0$ up to $z = -L$ is almost identical. Therefore, to reduce the memory space and the computation time a 2D model of the electrostatic field obtained in the $z = -L/2$ plane is used during the simulation.

A comparison between the intensity of the electrostatic field in the two electrode configurations is shown in Figures 2 and 3. The analysis of the value of the component E_x of the electrostatic field along the two axes $x = 0$ and $y = 0$ shows the presence of an intense electrostatic field in a configuration with two plane electrodes. The position occupied by these electrodes along the $y = 0$ axis is represented in figure 3.b by a discontinuity at the E_x component of the electrostatic field.

B. Motion equation

The trajectory of the particles in the electrostatic separation zone is obtained by solving the equation of motion:

$$m\frac{d\vec{v}(x, y, z)}{dt} = \vec{F}_g + \vec{F}_{el}(x, y) - \vec{F}_{air}(v_x, v_y, v_z) \tag{3}$$

Equation (3) takes into account the influence of the gravitational force $\vec{F}_g$, the electrostatic force $\vec{F}_{el}(x, y)$ and the particle / air friction force $\vec{F}_{air}(v_x, v_y, v_z)$.

C. Gravitational force

In the separation zone the particles are subjected to a gravitational force defined by equation (4)

$$\vec{F}_g = m\,\vec{g} \tag{4}$$

where m [kg] represents the mass of the particle; $\vec{g}$ gravitational vector and the norm $g = 9.81$ m/s^2.

For a particle of known mass m, the intensity and direction of the gravitational force is constant throughout the electrostatic separation zone.

D. Electrostatic force

In this simulation the electrostatic force applied to a particle is predicted by a simple model defined by the equation

$$\vec{F}_{el}(x, y) = q\vec{E}(x, y) \tag{5}$$

where q [C] is the charge of the particle acquired by triboelectric effect and $\vec{E}(x, y)$ [V/m] the electrostatic field generated in the position occupied by the particle.

The choice of model (5) is based on the following simplifying assumptions:

1 - The quantity of charges acquired by a particle in a triboelectric process is located at the geometrical center of the particle;

2 - The quantity of this charge is assumed constant throughout the simulation period;

3 - The impact between the particle and the electrode of the installation has no effect on the quantity of charge acquired by a particle;

4 - The presence of charged particles in the electrostatic separation zone does not cause any distortion of the electrostatic field $\vec{E}$ generated by the electrodes of the installation.

E. Particle/air friction force

According to the law of Stocks, the viscous friction force applied to particles of spherical shape in motion in the separation medium represented by the air is proportional to the relative velocity of the particle.

$$\vec{F}_{air} = -6\pi\eta_{air}r\vec{v} \tag{6}$$

where r [m] represents the radius of the spherical particle; $\vec{v}$ the speed of the particle and η_{air} the dynamic viscosity coefficient of the air. To simulate the force applied to a particle of irregular shape, we used the radius of the spherical particle which has an equivalent surface.

F. Integration of equation of motion

Equation (3) is an ordinary differential equation. The numerical resolution of this equation requires the availability of some information on the initial position and velocity of the particles. In this paper, the numerical integration of the equation of motion (3) is performed by applying the Euler- Cromer method represented by the iterative scheme (7). This method provides an approximate solution of (3) at times $t_0, t_1, t_2, ... t_n$ equidistant in the simulation interval.

$$x^{n+1} = x^n + v_x^{n+1}\cdot\Delta t \qquad y^{n+1} = y^n + v_y^{n+1}\cdot\Delta t \qquad z^{n+1} = z^n + v_z^{n+1}\cdot\Delta t \tag{7.1}$$

$$v_x^{n+1} = v_x^n + a_x^n\cdot\Delta t \qquad v_y^{n+1} = v_y^n + a_y^n\cdot\Delta t \qquad v_z^{n+1} = v_z^n + a_z^n\cdot\Delta t \tag{7.2}$$

The method used in the integration of the motion equation is implemented as a module in the simulation program represented by the flowchart of figure 4. The execution of the program begins with an initialization of the simulation parameters and an import of the finite element electrostatic field model implemented in the PDE-tool library of the MATLAB software.
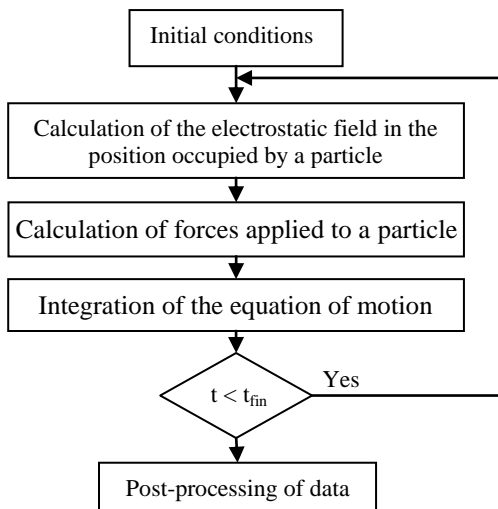

Fig. 4. Flowchart of the simulation program

In the second step, the simulation program calculates the intensity of the electrostatic field in the current position of the particle. This value is obtained from the numerical model of the electrostatic field. This information is used in the calculation of the electrostatic force applied to a particle. In this position the friction force between particles and air is calculated from the current velocity of the particle. The calculation of the sum of the forces applied to a particle allows the calculation of the acceleration of the particle from equation (3). In the next step the simulation program calculates the velocity and position of the particle after an integration time Δt by the Euler-Cromer method (7). The calculation continues as long as the current time is less than the final simulation time. The program then proceeds to the post processor data stage.

III. SIMULATION AND EXPERIMENTAL VALIDATION

An experimental study of particle trajectories in a free fall separator equipped with four cylindrical electrodes is carried out using a laboratory installation (Figure 1.b). The electrodes of the installation are made of PVC tubes the surface of which is covered by an adhesive aluminum ribbon. The axes passing through the centers of the electrodes are fixed in wooden supports which ensure the insulation and the adjustment of the position of the electrodes along the two axes Ox and Oy. The two electrodes on the right side of the installation are powered by a high voltage source (Figure 5.a) adjusted to -15 kV. The other two electrodes installed in the left side are powered by a voltage of +15 kV. The potential difference applied to the electrodes represents the maximum value that ensures the operation of the separator without the appearance of spark discharges between the electrodes. Once the high voltage is applied to the electrodes, the installation is continuously fed at a low flow rate with a granular mixture containing 50% PVC and 50% ABS. Before being introduced into the separator, the granular mixture is sorted according to the size of the particles using a stainless steel sieve (Figure 5.b). The sieving time is fixed at 5 min.
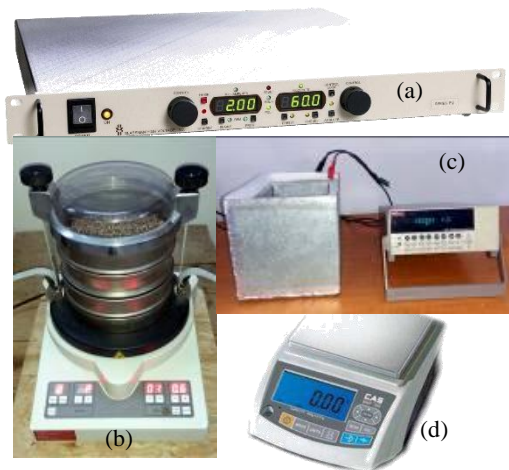

Fig. 5. Material used in the experimental work: (a) high voltage source; (b): sifter; (c) Faraday cage connected to an electrometer; (d): electronic balance (resolution 0.1 g).

TABLE 1: MASS OF RECOVERED PRODUCTS IN THE COLLECTOR
CELLS. DIAMETERS OF PARTICLES 1.4 mm $< Ø <$ 2.8 mm

	N°	Centre of cells	M_{exp} [g]	M_{sim1} [g]	M_{sim2} [g]
	1	-32.5	4.2	4.2	3.7
	2	-27.5	10.7	11.2	10.7
	3	-22.5	19.5	34.5	19.5
	4	-17.5	37.4	25.9	35.2
	5	-12.5	27.4	8.7	27.4
	6	-7.5	15.8	9.8	15.8
Position des cellules suivant Ox (cm)	7	-2.5	17.7	13.6	15.0
	8	2.5	18.9	17.4	17.7
	9	7.5	17.1	12.7	17.1
	10	12.5	24.6	12.5	24.6
	11	17.5	29.7	28.7	29.7
	12	22.5	21.0	24.3	15.8
	13	27.5	10.6	10.3	10.6
	14	32.5	4.2	3.0	3.1
	15	37.5	2.2	0.2	1.2
Degree of Concordance				82.30 %	99.22%

TABLE 2: CHARGE OF RECOVERED PRODUCTS IN THE COLLECTOR
CELLS. DIAMETERS OF PARTICLES 1.4 mm $< Ø <$ 2.8 mm

	N°	Centre of cells	Q_{exp} [nC]	Q_{sim1} [nC]	Q_{sim2} [nC]
	1	-32.5	-75.59	-82.89	-76.23
	2	-27.5	-210.04	-202.71	-192.13
	3	-22.5	-372.40	-559.67	-318.81
	4	-17.5	-536.31	-395.77	-536.41
	5	-12.5	-475.91	-115.43	-361.09
	6	-7.5	-232.36	-134.95	-221.03
Position des cellules suivant Ox (cm)	7	-2.5	-171.40	-150.68	-171.72
	8	2.5	144.23	136.40	144.34
	9	7.5	229.70	140.78	188.58
	10	12.5	291.30	137.19	272.80
	11	17.5	479.62	365.03	378.48
	12	22.5	245.46	376.00	245.80
	13	27.5	205.06	197.77	196.15
	14	32.5	77.78	77.87	78.41
	15	37.5	48.90	6.59	50.10
Degree of Concordance				93.83%	99.37%

Particles with a maximum diameter of between 1.4 mm and 2.8 mm recovered after sieving are introduced directly into the separator using a conical funnel with an outlet diameter of about 1 cm. The outlet of the funnel is installed in the center of the separation zone and its vertical position is adjusted to the upper level of the electrodes.

After separation, the charge and the mass of the product recovered in each cell of the collector are measured using a Faraday cage connected to an electrometer (Figure 5.c) and an electronic balance (Figure 5.d).

An image that shows the product recovered at the outlet of the separator is shown in figure 6.

Fig. 6. Products recovered in the collector cells (diameters of particles 1.4 mm < Ø < 2.8 mm)

The variation of the experimental values M_{exp} and Q_{exp} as a function of the positions along the axis Ox are compared with the values M_{sim} and Q_{sim} obtained by simulation of the trajectory of 6500 particles of average mass $m_p = 1/25$ g. This quantity is equivalent to 260 g of granular product which represents the total mass of the product used in the experimental work.

During the simulation we obtained different trajectories by the application of a set of parameters represented by: integration time $\Delta t = 0.01$ s; electrode radius $r_e = 0.1$ m; position of the electrode centers $(x, y) = (\pm 0.1$ m, ± 0.1 m); upper level of the electrodes $z = 0$ m; lower level of the electrodes $z = -1$ m; voltage applied to the electrodes $U = \pm 15$ kV; upper level of the collector $z = -1.2$ m; upper and lower limits of particle radius $(\mu_r, \sigma_r) = (0.85$ mm, 0.2 mm$)$; upper and lower limits of particle mass $(\mu_m, \sigma_m) = (1/25$ g, 1/100 g$)$; upper and lower limits of the charge/mass ratio of positive charge particles $(\mu_{Q/M+}, \sigma_{Q/M+}) = (15.10$ µC/kg, 4.82 µC/kg$)$; upper and lower limits of the initial velocity of the positively charged particles along the axis Ox, Oy and Oz $(\mu_{vx}, \sigma_{vx}) = (0.25$ m/s, 0.2 m/s$)$; $(\mu_{vy}, \sigma_{vy}) = (0$ m/s, 0.25 m/s$)$; $(\mu_{vz}, \sigma_{vz}) = (2$ m/s, 0.4 m/s$)$; upper and lower limits of the initial velocity of the negatively charged particles along the axis Ox, Oy and Oz $(\mu_{vx}, \sigma_{vx}) = (-0.25$ m/s, 0.2 m/s$)$; $(\mu_{vy}, \sigma_{vy}) = (0$ m/s, 0.25 m/s$)$; $(\mu_{vz}, \sigma_{vz}) = (-2$ m/s, 0.4 m/s$)$; upper and lower limits of the charge / mass ratio of the negatively charged particles $(\mu_{Q/M-}, \sigma_{Q/M-}) = (-13.12$ µC/kg, 3.48 µC/kg$)$; upper and lower limits of the initial position of the particles according to Ox $(\mu_x, \sigma_x) = (0$ cm, 0.5 cm$)$; upper and lower limits of the initial position of the particles along the axis Oy $(\mu_y, \sigma_y) = (0$ cm, 0.5 cm$)$; The charge of each particle is calculated from its charge/mass ratio and mass. These two parameters are considered as simulation parameters.

An overview of the particle trajectory obtained by the application of all these parameters is shown in figure 7.a. This figure shows the trajectory of 1000 particles and figure 7.b shows the behavior of a particle before and after an impact with one of the electrodes of the installation.
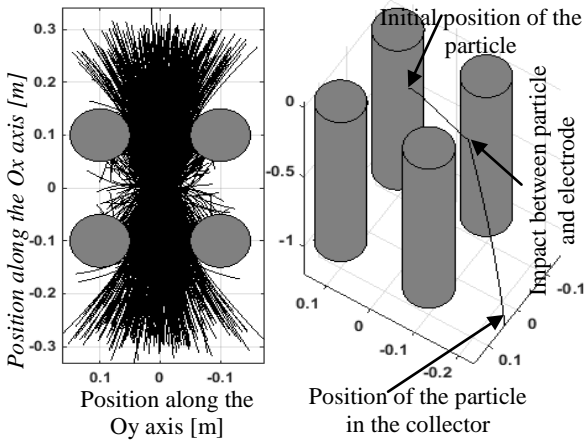
Fig. 7. Particle trajectories in a free fall separator; (a): Simulation of the trajectory of 1000 particles; (b) trajectory of a single particle.
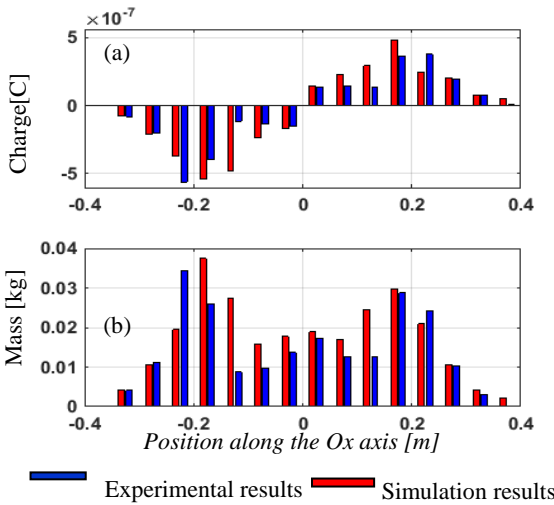

Fig. 8. Variation of the charge (a) and the mass (b) of the mass of the product recovered at the collector according to the position along the O*x* axis (first simulation).

The simulated values of the charge and mass distribution of a product quantity of 6500 particles as a function of the position at the collector of the installation are mentioned in column M_{sim1} and Q_{sim1} of Tables 1 and 2. The graphs associated with all these values are shown in figure 8. The curves in this figure show the presence of a difference between the values obtained by simulation and that obtained experimentally. The difference between these two values can be evaluated by the degree of concordance:

$$\text{deg} = 1 - \frac{\displaystyle\sum_{i=1}^{N}(\hat{y}_i - y_i)^2}{\displaystyle\sum_{i=1}^{N}\left[|\hat{y}_i - \bar{y}| + |y_i - \bar{y}|\right]^2} \tag{8}$$

where, y_i represents the measured value of the response in cell i; $\bar{y}$ the average of the measured values of the response y_i ; $\hat{y}_i$: the value of the response obtained by simulation in cell i; N: number of cells.

The degree of concordance between M_{sim1} and M_{exp} is 82.30%. In the same way, the agreement between Qsim1 and Q_{exp} is characterized by a degree 93.83%. To reduce the difference between simulation and experimental values we have created a database that contains information about the trajectories of 65000 particles. This is equivalent to 10 times the amount of the product used in the experimental study. In the second step we classified the particles of the database according to their positions in the collector cells. After the discrimination, we got 15 groups of particles. In the third step, we selected a random number of particles from the first group. The selection is made so that the total mass and the charge of the selected particles are as close as possible to the measured mass and load of the product recovered in the first cell of the collector. This step is repeated for all other groups of particles. The results obtained by the application of this method are shown in the column M_{sim2} and Q_{sim2} in Table 1 and Table 2.

Compared with the results of figure 8, the curves of figure 9 associated with the values of M_{sim2} and Q_{sim2} show a diminution of the difference between the experimental and simulated distributions. The concordance of these values with the experimental results is characterized by degrees higher than 90%.

IV. DISCUSSION OF RESULTS

From the histograms of each parameter (Figure 10), the charge of the particles used in the simulation must follow an extreme value distribution law the mathematical form of which is represented by:

$$f(x|k,\mu,\sigma) = \left(\frac{1}{\sigma}\right)\exp\left[-\left(1 + k\frac{(x-\mu)}{\sigma}\right)^{-\frac{1}{k}}\right]\left(1 + k\frac{(x-\mu)}{\sigma}\right)^{-1-\frac{1}{k}} \tag{9}$$

The distribution of masses and radii of particles both follow a normal distribution law:

$$f(x|\mu,\sigma) = \left(\frac{1}{\sigma\sqrt{2\pi}}\right)\exp\left(-\frac{(x-\mu)^2}{2\sigma^2}\right) \tag{10}$$

After adapting the parameters of the simulation model, we examined the particle mass distribution in different planes z = -0.1 m; -0.3 m and -1 m. The results obtained are shown in figure 11. The entire product can be collected at the center of the installation at a height of z = -0.1 m. In a low level z = -0.3 m, two separate zones are formed which means that the totality of the product can be collected around two different points (x, y) = (-0.05 m, 0 m) and (x, y) = (0.05 m, 0 m); at z = -1 m, all of the two products can be recovered around the points (x, y) = (-0.1 m, 0 m) and (x, y) = (0.1 m, 0 m).
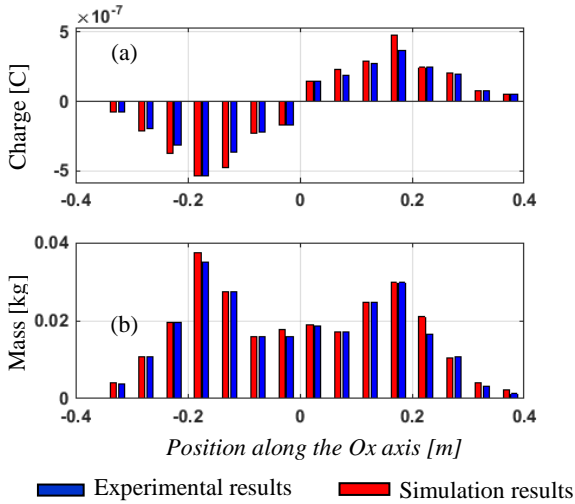
Fig. 9. Variation of the charge (a) and the mass (b) of the product recovered at the collector according to the position along the O*x* axis (second simulation).

The displacement of the collection points along the axis O*x* is accompanied by a dispersion of the granular product in both directions along the axis *Oy*. The analysis of the distribution of the charge / mass ratio of the particles recovered at this level shows that the selection of the highly charged particles must be carried out at the ends of the collector and in the vicinity of the electrodes.
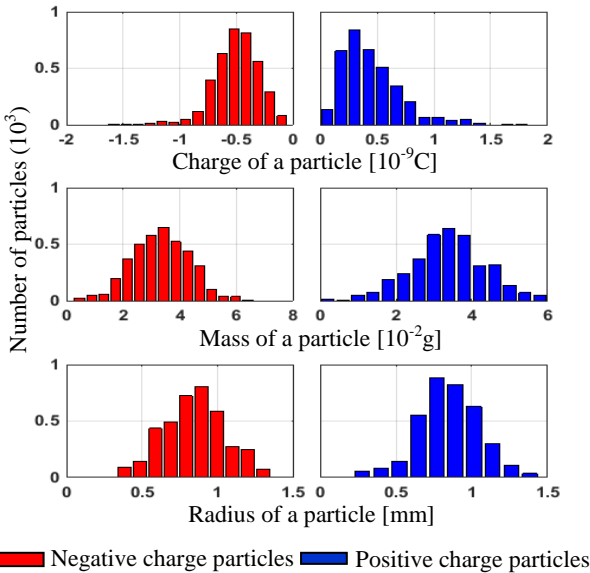

Fig. 10. Distribution of the parameters obtained after adaptation of the simulation results to all the experimental results
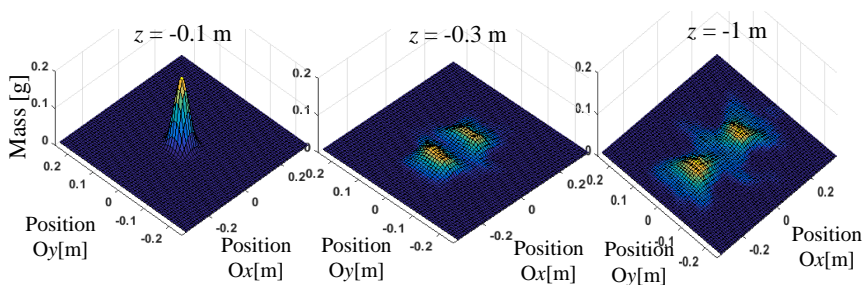
Fig. 11. Spatial distribution of the collected particles, at three different positions on the vertical axis of the separator (simulation results).

V. CONCLUSION

The intensity of the electrostatic field is higher in installations equipped with flat electrodes. Therefore, the highly charged particles are usually projected onto inappropriate cells of the collector after an impact with the electrode of the installation.

The results of the simulation as well as the experimental results obtained on a system equipped with cylindrical electrodes show that the number of collisions is reduced and the purity of the collected products increased. To reduce even more the change of particle direction after impact with one of the cylindrical electrodes, the authors propose the use of elliptical shaped electrodes. This solution which is the object of a future work makes it possible to increase the intensity of the electrostatic field in the center of the zone of separation and to reduce the angle between the trajectory of the particle and the surface of the electrode in the impact point which reduces abrupt changes in the trajectory after collision.

This work can be extended by: 1- A study based on the visualization of the trajectories to better understand the kinematics of the particles in this installation; 2- The development of a method that ensures the selection of an optimal set of trajectories from a database that includes several trajectories generated by parameters that represent an estimate of the real parameters. The optimal combination of several trajectories should minimize the difference between the experimental mass and the mass of the selected particles as well as between the experimental charge and the charge of the selected particles.

REFERENCES

[1] A. D. Moor, "*Electrostatics and its applications*", New York: Wiley, 1973.
[2] A. Tilmatine and L. Dascalescu, "Set-point identification of a free-fall electrostatic process for plastic particles", *Int. J. Environ. Stud.,* vol. 67, pp. 27-40, 2010.
[3] J. Wei, and M. J. Realff, "Design and optimization of free-fall electrostatic separators for plastics recycling", *AIChE J.* vol. 49, no. 12, pp. 3138–3149, 2003.
[4] S. Bendimerad, A. Tilmatine, M. Ziane, and L. Dascalescu, "Plastic wastes recovery using free-fall triboelectric separator", *Int. J. Environ. Stud.* vol. 66, pp. 529–538, 2009.
[5] L. Calin, A.Mihalcioiu, A. Iuga, and L. Dascalescu, "Fluidized bed device for plastic granules triboelectrification", *Part. Sci. Technol.*, vol. 25, no. 2, pp. 205–211, 2007.

[6]   A. Iuga, L. Calin, V. Neamtu, A. Mihalcioiu, and L. Dascalescu, "Tribocharging of plastics granulates in a fluidized bed device", *J. Electrostat.*, vol. 63, no. 6–10, pp. 937–942, Jun. 2005.

[7]   L. Dascalescu, A. Urs, S. Bente, M. Huzau, and A. Samuila, "Charging of mm-size insulating particles in vibratory devices", *J. Electrostat.*, vol. 63, no. 6–10, pp. 705–710, Jun. 2005.

[8]   M. Blajan, R. Beleca, A. Iuga, and L. Dascalescu, "Triboelectrification of granular plastic wastes in vibrated zigzag-shaped square pipes in view of electrostatic separation," *IEEE Trans. Ind. Appl.*, vol. 46, no. 4, pp. 1558–1563, Jul./Aug. 2010.

[9]   S. Masuda, M. Toragushi, T. Takahashi, and K. Haga, "Electrostatic beneficiation of coal, using a cyclone-tribocharger". *IEEE Trans. Ind. Appl.*, vol. 19, pp. 789-793, 1983.

[10]   M. Ha, C. Jeon, D. Choi, and H. Choi, "A numerical study on the triboelectrostatic separation of PVC materials from mixed plastics for waste plastic recycling". *J. Mech. Sci. Technol.*, vol. 17, pp. 1485–1495, 2003.

[11]   A. Younes, M. Younes, H. Sayah, A. Samuila and L. Dascalescu, "Experimental and Numerical Modeling of a New Tribo-Electrostatic Separation Process for Granular Plastics Mixtures", *Particulate Science and Technology*, vol. 33, no. 2, pp. 189-196, 2015.

[12]   L. Calin, A. Mihalcioiu, S. Das, V. Neamtu, C. Dragan, L. Dascalescu, A. Iuga, "Controlling Particle Trajectory in Free-Fall Electrostatic Separators", *IEEE Trans. Ind. Appl.*, vol. 44, pp. 1038-1044, 2008.

[13]   H. Labair, S. Touhami, A. Tilmatine, S. Hadjeri, K. Medles, L. Dascalescu, "Study of charged particles trajectories in free fall electrostatic separators", *J. Electrostat.*, vol. 88, pp. 232-235, 2017

[14]   M. Saeki, "Triboelectric separation of binary plastic mixture", *World Academy of Science, Engineering and Technology*, vol. 4, pp. 795-798, 2010.